Journal of Cellular Biochemistry 94:744–762 (2005)

Vanadium Induces Apoptosis and Modulates the Expressions of Metallothionein, Ki-67 Nuclear Antigen, and p53 During 2-Acetylaminofluorene-Induced Rat Liver Preneoplasia

Tridib Chakraborty, Shaonly Samanta, Balaram Ghosh, N. Thirumoorthy, and Malay Chatterjee*

Department of Pharmaceutical Technology, Division of Biochemistry, Jadavpur University, PO Box 17028, Calcutta 700032, India

Abstract Our previous studies have shown that vanadium, a dietary micronutrient, has an inhibitory effect against experimentally induced rat hepatocarcinogenesis. In this study, we evaluated the role of vanadium on some potential protein expression markers of carcinogenesis, such as metallothionein (MT), an intracellular metal-binding protein linked with cell proliferation and apoptosis, Ki-67 nuclear antigen, and p53 tumor suppressor during 2-acetylaminofluorene (2-AAF)-induced (0.05% in basal diet) rat liver preneoplasia. In a short-term regimen, supplementation of vanadium at a dose of 0.5 ppm effectively suppressed the formation of DNA 'comets' (29.55%; $P < 0.02$), thereby indicating its nongenotoxicity at this particular dose. Vanadium administration throughout the study reduced relative liver weight (RLW), nodular incidence (57.15%), total number, and multiplicity (48.45%) with restoration of hepatic zinc (Zn), magnesium (Mg), selenium (Se), copper (Cu), iron (Fe), and calcium (Ca) contents when compared to the carcinogen control. Moreover, treatment with vanadium significantly abated the expressions of MT and Ki-67, studied at four sequential time points. An increased immunopositivity of p53 protein ($1.03 \pm 0.23\%$; $P < 0.02$) was found in vanadium-treated rat liver with an elevated apoptotic-labeling index (AI; $P < 0.001$) as documented by TUNEL assay. Furthermore, a positive correlation between MT expression and Ki-67 labeling along with a strong negative correlation between MT immunoreactivity and AI ($r = -0.9000$, $P = 0.0004$ at week 24) at various time intervals suggest that, vanadium-mediated suppression of MT and Ki-67 expressions may be associated with induction of apoptosis. The results thus provide evidence for the first time in support of the potential role of vanadium on induction of p53 and apoptosis with concurrent suppression of MT and Ki-67 in order to have an understanding, in part, of the chemopreventive mechanism of this trace element in limiting neoplastic transformation in a defined model of experimental rat hepatocarcinogenesis. J. Cell. Biochem. 94: 744–762, 2005. © 2004 Wiley-Liss, Inc.

Key words: 2-acetylaminofluorene; hepatocarcinogenesis; preneoplastic lesions; vanadium; DNA-strand breaks; metallothionein; Ki-67; p53; apoptosis

In recent years, research on the biological influence of micronutrients in cancer has grown enormously. Among these, vanadium, a non-platinum trace metal has received considerable attention as an antitumor agent [French and Jones, 1993]. Vanadium influences the behavior of enzymes, mimics growth factor activity, and regulates gene expression [Stern et al., 1993]. The unique cellular activity of vanadium makes it a tool of unparalleled potential for studying mechanisms of cell growth, differentiation, and metabolism. Vanadium compounds have been found to be potentially effective against murine leukemia, fluid and solid Ehrlich ascites tumor [Kopf-Maier and Kopf, 1988], and mammary adenocarcinoma [Murthy et al., 1988]. Sakurai et al. [1995] have found strong antitumor chemopreventive activities of vanadyl complexes of 1,10-phenanthroline [$VO(Phen)^{2+}$] and related derivatives against human nasopharyngeal carcinoma and the observed effects

Grant sponsor: University Grant Commission (UGC), Government of India; Grant number: P-1/RS/34/2001.

*Correspondence to: Dr., Prof. Malay Chatterjee, Department of Pharmaceutical Technology, Division of Biochemistry, Jadavpur University, PO Box 17028, Calcutta 700032, India. E-mail: mcbiochem@yahoo.com

Received 8 June 2004; Accepted 6 August 2004

DOI 10.1002/jcb.20304

© 2004 Wiley-Liss, Inc.

were found to be superior than the chemotherapeutic drug, *cis*-diamminedichloroplatinum. 2-Acetylaminofluorene (2-AAF) is a complete hepatocarcinogen in rats forming DNA-carcinogen adducts and inducing DNA-strand breaks and in turn hepatocellular carcinomas (HCCs) without cirrhosis through the development of putative preneoplastic enzyme-altered focal lesions [Tatematsu et al., 1988; Saha et al., 2001].

Since its introduction in 1970, the technique of proton-induced X-ray emission (PIXE) spectrometry has been successfully used by various groups throughout the world for trace element analysis of biomedical samples [Feldstein et al., 1998]. PIXE forms a powerful analytical tool due to high sensitivity, multi-elemental analysis at a time and its non-destructive nature. The advantage of PIXE analysis in studying physiologically important elements, such as zinc (Zn), magnesium (Mg), iron (Fe), copper (Cu), selenium (Se), etc. is that, it not only allows precise quantitative elemental analysis but can also demonstrate the minute differences in the cellular distribution pattern of trace elements of normal and pathological tissues.

The tissue levels of biologically essential trace elements are an important factor in disease progression as they play a key role in maintaining the chromatin structure and thereby genomic stability [Fenech and Ferguson, 2001]. It is, therefore, reasonable to assume that, alteration in ionic homeostasis would increase the possibility of altered molecular signaling events leading to enhanced and/or reduced cell proliferation and apoptosis and thus may exert its impact on the expression of a premalignant phenotype.

Carcinogen-induced alterations of the DNA helix include helical distortion, single-strand breaks (SSBs), double-strand breaks (DSBs), inter-strand crosslinks, and chromosomal aberrations [Lindahl, 1993]. The magnitude of DNA SSBs is a measure of genotoxicity following carcinogen exposure. The inability of cells to repair such damage adequately is a putative causal event in chemical carcinogenesis. Single cell gel electrophoresis (SCGE) or comet assay, the alkaline version in particular has become a very popular method for analysis, detection, and measurements of DNA damages caused by various chemical and physical agents, including DNA SSBs, alkali-labile damage, and excision repair sites in an individual cell in interphase [Qiu et al., 2003].

The basal expression of metallothionein (MT) in normal cells has generally been associated with heavy metal detoxification, intracellular trace elements storage, and scavenging of free radicals [Huang and Yang, 2002]. Up-regulation of MT expression in rapidly proliferating tissues appears to suggest its critical role in normal and neoplastic cell growth. MT overexpression has been linked with enhanced cell proliferation in squamous cell carcinoma of the esophagus, ovarian cancer, breast cancer, and nasopharyngeal cancer [Oyama et al., 1996; Jayasurya et al., 2000]. Besides, the expression of the nuclear proliferating antigen Ki-67 and its presence during all active phases of the cell cycle but not in resting cells makes it an excellent marker for neoplasia [Ito et al., 1999]. The fraction of Ki-67-positive tumor cells is often correlated with the clinical course of the disease.

The tumor suppressor protein p53 is one of the most frequently activated proteins in apoptosis. p53 is able to respond to different cellular stresses, such as DNA damage, hypoxia, and oxidative stress. As a critical cellular mediator, p53 has a direct role in maintaining the integrity of the genome. Loss of p53 activity has been associated with tumor progression and unfavorable prognosis of the tumor [Symonds et al., 1994].

Previous studies from our laboratory have shown that, supplementation of 0.5 ppm vanadium in drinking water was quite effective in suppressing diethylnitrosamine (DEN)-induced hepatocarcinogenesis in rats without any toxic manifestations. The suppressive effect of vanadium has been reflected in hematological and histopathological indices [Bishayee et al., 1997], selective induction and stabilization of hepatic xenobiotic biotransforming enzymes [Bishayee et al., 1999], in DEN-evoked chromosomal damage and DNA-strand breaks in rat hepatocytes [Basak et al., 2000] and in sister-chromatid exchanges and DNA–protein cross-link formations with restoration of antioxidants during 2-AAF-induced rat hepatic preneoplasia [Chakraborty et al., 2003].

This study was undertaken to have an understanding of the roles of alterations of hepatic levels of trace elements and significance of the expressions of MT and Ki-67 proteins as important markers of carcinogenesis in the development of premalignant phenotype and the reported dose (0.5 ppm) of vanadium in

suppressing 2-AAF-induced carcinogenicity. Several reports are available to show that, overexpression and up-regulation of MT and Ki-67 proteins are associated with the carcinogenic process. But, to our knowledge, reports documenting the antineoplastic potential of chemopreventive agents in modulating these indices are meager. This is for the first time we are reporting the chemopreventive potential of vanadium in suppressing MT and Ki-67 expressions in preneoplastic rat liver. The study further focuses the role of vanadium on p53 expression and induction of apoptosis in a defined rat model of experimental hepatocarcinogenesis.

MATERIALS AND METHODS

Materials and Maintenance of Animals

All the reagents and biochemicals, unless otherwise mentioned were obtained from Sigma Chemicals Co. (St. Louis, MO), and E. Merck (Franfurter Straße, Darmstadt, Germany).

Male Sprague–Dawley rats obtained from the Indian Institute of Chemical Biology (CSIR), Kolkata, India weighing 80–100 g at the beginning of the experiments were used throughout the study. The animals were acclimatized to standard laboratory conditions (temperature $24 \pm 10^{\circ}$C, relative humidity $55 \pm 5\%$ and a 12 h photoperiod) in Tarson Cages (four to five rats per cage) for 1 week before the commencement of the experiment. During the entire period of study, the rats were supplied with a semi-purified basal diet (Lipton India Ltd., Mumbai, India) and water ad libitum. The recommendations of Jadavpur University's "Institutional Animal Ethics Committee" ["Committee for the Purpose of Control and Supervision of Experiment on Animals" (CPCSEA Regn. No. 0367/01/C/CPCSEA) India] for the care and use of laboratory animals were strictly followed throughout the study.

Experimental Regimen

Rats were randomly divided into four experimental groups as illustrated in Figure 1. Groups B and D rats were the 2-AAF-treated groups that started receiving 2-AAF at 9 weeks of age, i.e., at week 4 of experimentation, at a dose of 0.05% in basal diet, once daily for 5 days a week for 28 consecutive weeks, i.e., till week 32. Group A and B rats were the normal and 2-AAF controls, respectively. Group C (vanadium control) and D (vanadium + 2-AAF) rats received 0.5 ppm vanadium (w/v) as ammonium monovanadate (NH_4VO_3, +V oxidation state) in drinking water, ad libitum starting 4 weeks prior to 2-AAF administration and continued thereafter along with 2-AAF till the sacrifice of the animals (i.e., upto 32 weeks). Solutions of vanadium (pH 7.0) were renewed every 2–3 days. Daily food and water intakes were noted and the body weights of the animals from each group were recorded every second day. All the treatments were withdrawn after week 32 and the rats were sacrificed by decapitation between 09:00 and 11:00 h under proper light ether anesthesia after week 33 to carry out experimentations. All the animals were fasted over night before sacrifice. For immunohistochemistry, four sets of rats comprising of all the above four groups were maintained and were sacrificed at four different time points, i.e., after 8, 16, 24, and 32 weeks from the starting of the experiment. For estimation of DNA-strand breaks, all the rats were killed after the last feeding of 2-AAF at day 40, livers were promptly excised and hepatic DNA was isolated.

Histo-Morphometry of Liver Tissue

After the rats were sacrificed, their livers were promptly excised, blotted, weighed dried, and then examined macroscopically on the surface as well as in 3 mm cross sections for gross visible persistent nodules (PNs), which represented focal proliferating, hepatic lesions with a low tendency to spontaneous regression. The PNs were divided into three categories, in accordance with their respective diameter and total area of liver parenchyma occupied, namely, ≥ 3, < 3 to ≥ 1, and ≤ 1 mm [Moreno et al., 1991]. Formalin-fixed tissue sections of 5 μM in thickness were cut, stained with hematoxylin and eosin (H&E) and observed under an ADCON-5591 photomicroscope for routine hepatic histopathology.

PIXE Analysis of Liver Samples

Sample selection and preparation. The liver tissues were dissected out from all the control and experimental groups and were washed for 2 h in acetone, then with double distilled water followed by acetone and finally rinsed in distilled water to remove surface contaminations. The samples were then dried for about 3–4 h in a quartz container at 65–70°C to avoid

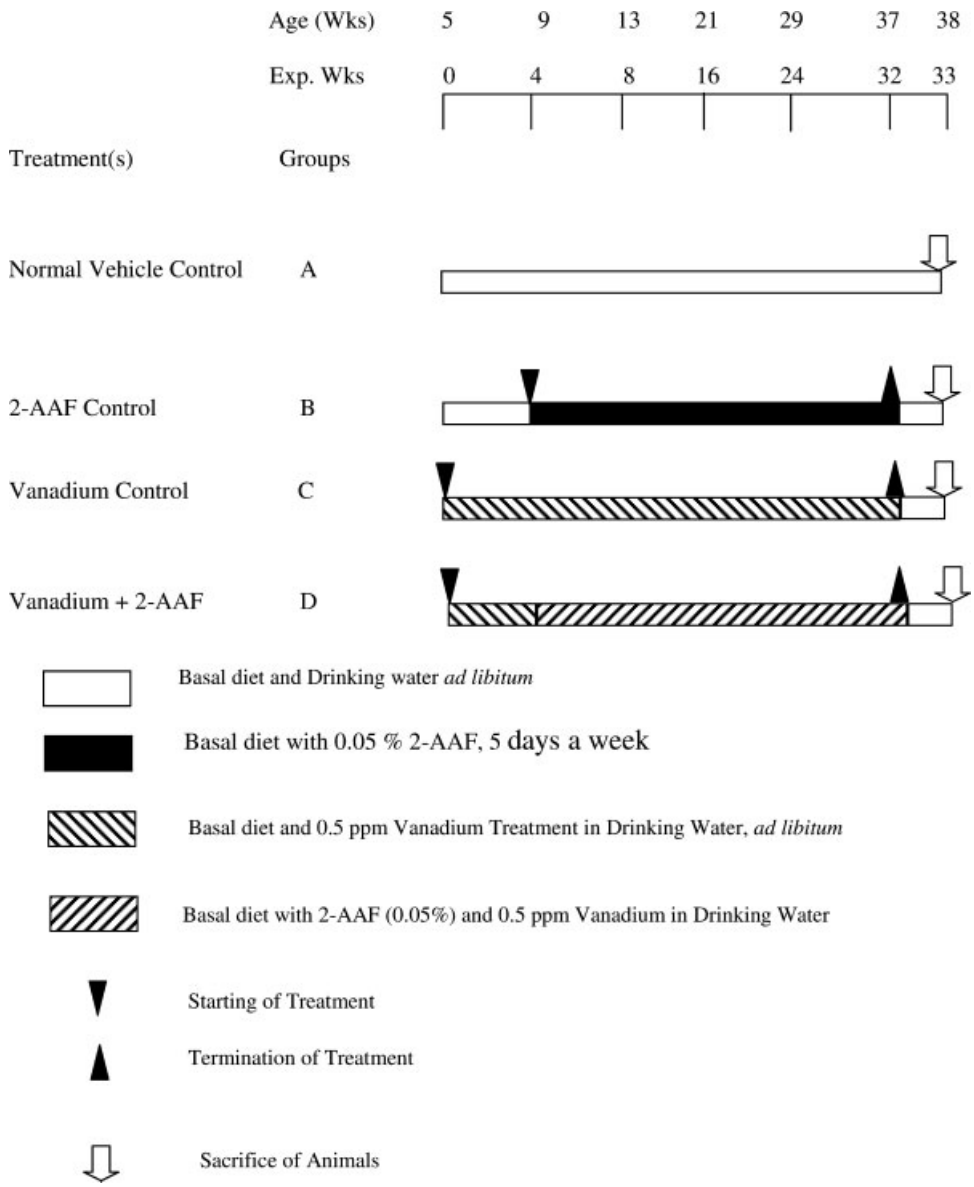

Fig. 1. Basic experimental protocol for histo-morphometry, metal estimations, and immunohistochemistry.

carbonization. Then the samples were lyophilized, ground into fine powder with a glass mortar and pestle and finally pressed into pellets. Conversion of the sample into fine powder before pelletization is necessary to avoid particle size effects during analysis. These effects are particularly important for the lighter elements. To obtain consistent pellets, which remain stable during bombardment, an equal amount of binder such as graphite was added to the powdered sample prior to pelletization so that the pellet is made conductive and that bombardment in vacuum does not lead to charging of the specimen. The diameter and mass of each pellet were made 13 mm and 300 mg, respectively [Kwiatek et al., 1987].

Target irradiation. High voltage protons of 3 MeV, obtained from the 3 MV low-energy tandem pelletron electrostatic accelerator, collimated to a beam of 3-mm diameter were used to irradiate the targets. The targets were mounted in a target holder. Then the target holder was loaded into the PIXE chamber and the irradiation was carried out under vacuum (10^{-6} Torr). The target holder can be moved in the vertical direction, which allows the analysis of different targets without changing the irradiation and measuring geometry. The target is

positioned in such a way, that the solid angle subtended between (i) the target and the beam, and (ii) the target and the detector is maximum and optimum.

Data acquisition for PIXE. An energy-dispersive Si (Li) detector (EG and G ORTEC) with a full-width at half-maximum FWHM (energy resolution) of 170 eV at 5.9 KeV (active area 30 mm^2 placed at 90° with respect to the incident beam direction), beryllium window of 8 μm thickness and a long cryostat of 22 cm length were used (Canberra Industries, Inc., Meriden, CT) to detect the characteristic X-rays emitted from the targets [Hota et al., 2001]. The target holder is mounted on an insulated stand-off and is surrounded by a cylindrical electron suppressor held at negative potential with respect to the target. Integrated charge on the target was measured using a current integrator, which was connected to the target holder. X-rays leave the PIXE chamber through a 25 μM Mylar window and traverse approximately of 1 cm air gap before entering the detector. A 350 μM thick Mylar absorber was kept in front of the detector to attenuate high electron Bremsstrahlung background and intensities of dominant low-energy X-ray peaks. The beam current was adjusted for maximum yield (about 5 nA) and the counting rate was kept below 1,000 cps. Canberra spectroscopy amplifier, Model no. 2020 was used for signal amplification. The X-ray yield seen through the Si (Li) detector was collected using the Canberra series 88 Multi Channel Analyzer [Hota et al., 2001]. The data was then transferred to the MICROVAX II DEC SYSTEM and then PC At 486 EISAQ computer for quantification of elemental concentrations present in the sample.

Data analysis. Thick target PIXE analysis was performed using the GUPIX-95 software, which provides non-linear least squares fitting of the X-ray spectrum through an AXIL program, together with subsequent conversion of the X-ray peak intensities into respective elemental concentrations via a defined standardization technique involving fundamental parameters and user-defined instrumental constant [Maxwell et al., 1995]. Full account was taken for the matrix effects and secondary fluorescence contributions in both the spectrum fitting portion and the calculation of concentrations.

For a given target (i.e., sample, standard or reference material) the measured intensity or yield of proton-induced X-rays in the principal X-ray line Y (Z, M) for an element Z in a matrix M can be written:

$$\mathrm{Y}(\mathrm{Z},\mathrm{M}) = \mathrm{Y1t}(\mathrm{Z},\mathrm{M}) \times \mathrm{Cz} \times \mathrm{Q} \times \mathrm{fq} \times (\mathrm{omega}) \times (\mathrm{eff}) \times (\mathrm{trans}) \quad (1)$$

where Y1t is the computed theoretical intensity or yield per micro-Coulomb of beam charge per unit concentration per steradian for the particular matrix; Cz is the actual concentration of Z in M; omega is the detector front face solid angle in steradians; Q is the measured beam charge or quantity proportional thereto; if the latter, then fq converts Q to micro-Coulombs; if the former then fq is 1.0 assuming proper electron suppression at the target; eff is the intrinsic efficiency of the Si (Li) detector; (close to 1.0 between 5 and 20 keV); and trans is the X-ray transmission through any filters or absorbers between target and detector.

Combining fq and omega into an instrumental constant H subsumes both the Si (Li) detector solid angle and any calibration for intrinsic to whatever device is used to integrate the beam current. When the standardization option is requested in GUPIX, the equation:

$$\mathrm{Cz} = \frac{\mathrm{Y}(\mathrm{Z},\mathrm{M})}{\{\mathrm{Y1t}(\mathrm{Z},\mathrm{M}) \times \mathrm{H} \times \mathrm{Q} \times \mathrm{eff} \times \mathrm{trans}\}} \quad (2)$$

is solved to convert measured X-ray yield to concentration for all elements fitted.

Estimation of Hepatic DNA Damage (DNA-Strand Breaks) by Comet Assay

Hepatic DNA-strand breaks (tailed DNA) were measured in liver samples using the alkaline Comet assay essentially as described by Olive et al. [1992]. The tissues were smoothly homogenized in phosphate buffered saline (PBS) (2.7 mM KCl, 8.1 mM Na_2PO_4, 1.5 mM KH_2PO_4, and 0.14 mM NaCl; pH 8.0) under refrigeration and filtered. Cell viability was determined by the trypan blue method. Four microliters of the homogenized tissue was then transferred to 50 μl of fresh PBS (pH 7.5), washed, and suspended in 150 μl of 1% low melting point agarose at 37°C prepared in PBS and pipetted onto an agarose-precoated glass microscopic slide. After keeping the slide on a chilled plate for 10 min, the slide was immersed in fresh ice-cold lysis solution (2.5 M NaCl, 0.1 M Na_2EDTA, 10 mM Tris-HCl [pH 10], 10% DMSO, and 1% Triton X-100) at 4°C in the dark for 60 min, washed, and then the slide was placed in a horizontal

electrophoresis tank containing freshly made buffer (0.3 M NaOH and 1 mM Na_2EDTA, pH >13) for 40 min at 4°C. Electrophoresis was performed in the same buffer for 30 min at 0.8 V/cm and adjusting the current to 300 mA by slowly changing the buffer level. After electrophoresis, the slide was rinsed gently with 0.4 mM Tris-HCl (pH 7.5) for 5 min, stained with ethidium bromide (5 μg/ml), and viewed under a Zeiss fluorescence microscope equipped with a green excitation filter and a 590 nm barrier filter. Routinely 150 cells (50 cells/slide) were screened per sample. Nucleoid DNA extends under electrophoresis to form 'comet tails,' and the length of the comets was evaluated using a computerized image analysis system for determination of the percentage of tailed DNA that is linearly related to the frequency of DNA-breaks.

Immunostaining of MT, Ki-67, and p53

Immunohistochemical detection of MT, Ki-67 nuclear antigen, and p53 proteins in cold acetone-fixed, paraffin embedded liver sections was performed by the avidin–biotin–peroxidase-complex method [Jin et al., 2002]. Briefly, 5 μM thin sections on lysine-coated slides were deparaffinized and rehydrated. Endogenous peroxidase activity was blocked with 1% H_2O_2 in 0.1 M Tris-NaCl (pH 7.6) for 30 min. After incubation with 5% normal goat serum for 1 h at 37°C, sections were incubated overnight at 4°C with the primary antibody rabbit antirat MT-1 (a kind gift) in 1% BSA using a 1:50 dilution. Sections were then incubated with a biotinylated secondary antibody goat antirabbit IgG (Sigma) for 30 min at 37°C with 1:200 dilution. This was followed by incubation with streptavidin peroxidase (1:100) for 1 h and subsequent chromagen development with 0.5% 3,3′-diaminobenzidine tetrahydrochloride (DAB) and 0.33% H_2O_2 in 0.5M Tris-NaCl as the substrate. The sections were then counterstained with Harris hematoxylin, dehydrated and mounted and served as positive control. Negative controls were prepared following all the above-mentioned steps omitting the primary antibody. For Ki-67 and p53 immunolabeling, antigen retrievals were facilitated by heating the sections in citrate buffer (pH 6.0) for 20 min before quenching of endogenous peroxidase. After incubation in normal goat serum, sections were then separately incubated with the respective primary antibodies, mouse antirat Ki-67 (MIB5) (Dako Corporation, Carpenteria, CA) and sheep anti-p53 antibody (Sigma) at 1:100 and 1:300 dilutions, respectively. The rest of the steps were similar to the protocol for MT immunohistochemistry. MT, Ki-67, and p53 immunostainings were considered positive when the nuclei (for all) and cytoplasm (for MT) of the hepatocytes were stained prominently purplish brown/reddish brown. MT immunoreactivity and Ki-67 labeling index (KI) were expressed as percentage of immunopositive cells. A total of ten high power fields were randomly chosen. The number of +ve cells was determined in relation to the total number of cells in that field.

In Situ Detection of Apoptosis by TUNEL Assay

Apoptotic cells in paraffin sections were detected by the terminal deoxynucleotidyl transferase (TdT)-mediated deoxyribonucleotide triphosphate (dUTP) nick end labeling (TUNEL) method [Gavrieli et al., 1992]. Briefly, paraffin sections were permeabilized with proteinase K (20 μg/ml) for 15 min after deparaffinization and rehydration. Endogenous peroxidase was inactivated by treating with 3% H_2O_2. After equilibration with TdT buffer (pH 7.2), the sections were end-labeled with biotinylated 16-dUTP (0.04 nmol/μl; Boehringer) in TdT reaction solution for 2 h at 37°C, and labeled cells were detected using streptavidin–horseradish peroxidase (HRP) conjugate. The chromagen substrate DAB reacts with the bound enzyme to generate an intense signal of brown color at the sites of DNA fragmentation. Finally, the sections were counterstained with methyl green. Quantitative evaluation of apoptotic cells was done by examining the sections in ten random fields and counting the number of TUNEL-positive cells in those sections. The apoptotic index (AI) was expressed as TUNEL-positive cells per 100 cells.

Statistical Analysis

The data were analyzed using the GraphPad Prism software package, Version 4.01. Student's *t*-test was performed to compare sample means and the results were expressed as mean ± SE. One-way ANOVA followed by Tukey–Kramer multi-comparison test was also performed to evaluate the changes among different time intervals within a variable using the error calculated from ANOVA. Pearson's correlation was used to analyze the relationship

between variables. Statistical significance was set at $P < 0.05$ for all the values.

RESULTS

During the entire period of study, no differences in food and water consumption were observed among the various groups of animals. Food and water intakes were 10.7–12.8 g 100 g^{-1} day^{-1}, and 8–10 ml/day/rat, respectively, for all rat groups. Six rats from different experimental groups died before the end of the study (i.e., 32 weeks): four from Group B (26.66%) and one each from Group C (10%) and Group D (6.66%).

Body and Liver Weight

Table I shows the final body weight, liver weight, and relative liver weight (RLW) of different groups of rats that were killed after 32 weeks of the study. The final body weight of 2-AAF control rats (Group B) was significantly less ($P < 0.0001$) than that of the normal vehicle control (Group A). In Group C (vanadium control), supplementation of 0.5 ppm vanadium for 32 consecutive weeks maintained the body weight at the normal level and there was no significant differences between Group A (normal vehicle control) and Group C (vanadium control) suggesting that vanadium supplementation in this study had practically no adverse effect on the growth responses of the rats. Treatment with vanadium significantly increased ($P < 0.0001$) the final body weight of Group D rats compared to the carcinogen control (Group B). There was no significant difference among the groups in their liver weights. On the other hand, the RLW of Group B rats was found to be increased significantly ($P < 0.001$) compared to that of Group A. Vanadium treatment reduced the RLW in Group D rats ($P < 0.001$) when compared with Group A.

Effect of Vanadium on the Number and Size Distribution of Visible Hyperplastic Nodules in Rat Liver Treated With 2-AAF

There was no visible hepatocyte nodule in the livers of normal control (Group A) as well as vanadium control (Group C) groups. Table II summarizes the final nodular incidence, total number of nodules, and average number per nodule bearing liver of 2-AAF-treated groups in the presence or absence of vanadium after week 32. There was 100% nodular incidence in 2-AAF control rats. Supplementation of vanadium decreased the nodular incidence (57.15%) in the Group D rats that received vanadium for 32 successive weeks. There was also a decrement in the total number of nodules (71.79%) in Group D rats. There was a maximum occurrence of nodules $\geq$3 mm (23.07%) in 2-AAF control rats whereas there was no occurrence of this type of nodules in Group D. In the vanadium treated rats, the percentage of nodules ($\leq$1 mm) was increased (72.73%) when compared to the 2-AAF control rats. Also, the nodule multiplicity was decreased significantly ($P < 0.02$; 48.45%) in the 2-AAF treated rats when compared to the 2-AAF control.

Effect of Vanadium on Hepatic Architecture

Phenotypically altered hepatocyte populations including persistent nodules (PNs) were found scattered in the livers of 2-AAF-treated groups (i.e., Groups B and D) but no such alterations were noticeable in untreated normal control (Group A; Fig. 2A) or in the vanadium control (Group C). In Group B rats (Fig. 2B,C), a gross alteration in hepatocellular architecture was found and hepatocytes appeared oval or irregular in shape. The altered hepatocytes of foci and nodules were found to be consistently

TABLE I. Final Body Weight, Liver Weight, and Relative Liver Weight (RLW) of Different Groups of Rats Killed After Week 32

Group	Treatment(s)	Effective number of rats	Body weight	Liver weight	RLW
A	Normal control	10	319.74 ± 5.59	8.28 ± 0.26[a]	2.58 ± 0.05
B	2-AAF control	11	271.01 ± 2.99*	9.64 ± 0.57	3.55 ± 0.19**
C	Vanadium control	9	324.99 ± 3.57	7.82 ± 0.12	2.40 ± 0.06
D	Vanadium + 2-AAF	14	308.51 ± 4.86***	8.03 ± 0.25	2.61 ± 0.08[†]

[a]Values represent mean $\pm$ SE.
*$P < 0.0001$ when compared to normal control (Group A).
**$P < 0.001$ when compared to normal control (Group A).
***$P < 0.0001$ when compared to 2-AAF control (Group B).
[†]$P < 0.001$ when compared to 2-AAF control (Group B).

TABLE II. Effect of 0.5 ppm Vanadium on the Development of Nodular Hyperplasia in Rat Liver Treated With 0.05% 2-AAF

Group	Treatment(s)	Number of rats with nodules/total number of rats	Nodule incidence (%)	Inhibition (%)	Total number of nodules	Nodules relative to size (% of total number)			Nodule[a] multiplicity	Inhibition (%)
						≥3 mm	<3 to >1 mm	≤1 mm		
B	2-AAF	11/11	100.00	—	39	9 (23.07)	25 (64.10)	5 (12.82)	3.55 ± 0.58[b]	—
D	V + 2-AAF	6/14	42.85	57.15	11	0 (0.00)	3 (27.27)	8 (72.73)	1.83 ± 0.23*	48.45

[a]Average number of nodules/nodule bearing liver.
[b]Values represent mean ± SE.
*$P < 0.02$ when compared with 2-AAF control (Group B).

enlarged with more than one nucleus, which were moreover largely vesiculated with centrally located nucleoli. Some nuclei in the cells were large and hyperchromatic (basophilic), indicating prominent hyperbasophilic preneoplastic focal lesions around the portal vein that were clearly distinguishable from the surrounding non-nodular normal parenchyma. Extensive vacuolation was observed in the cytoplasm around the nucleus with masses of acidophilic (eosinophilic) material and a number of prominent clear cell foci. In contrast, the cellular architecture of hepatic lobules seemed to be almost like that of normal liver in Group D (Fig. 2D) that received vanadium supplementation during the entire period of study. Liver sections from this group presented only a few clear cell foci. The cells were generally filled with cytoplasmic material and were less vacuolated. The size of the nuclei was essentially the same as that of normal cells and cells with two nuclei were considerably fewer than in Group B.

Effect of 0.5 ppm Vanadium on the Hepatic Levels of Zn, Mg, Se, Cu, Fe, and Ca

Figure 3 shows a typical PIXE spectrum of different elemental peaks in vanadium treated liver sample (Group D). Mean concentration of six essential/trace elements in the different control and experimental groups of rat liver samples was measured by vacuum PIXE spectroscopy and shown in Table III. Results from this study show that, the elemental concentrations of Zn, Mg, and Se were significantly lower in the carcinogen control group (Group B) than the normal control (Group A), whereas Cu, Fe, and Ca showed elevated levels in the carcinogen control group, but the results were highly significant for the former two. In contrast, elemental analysis of tissue samples in the treatment group (Group D) exhibited marked closeness of all the elements to the normal values except for Ca, which showed an increased hepatic content ($P < 0.0001$) over carcinogen control as well as normal control.

Effect of Vanadium on Hepatic DNA-Strand Breaks in Rat Liver Following 0.05% 2-AAF Feeding

Figure 4 shows the extent of oxidative DNA damage in rat liver following 2-AAF exposure and its suppression by vanadium. The mean length to width (L:W) ratio of the DNA mass indicating the extent of DNA damage was

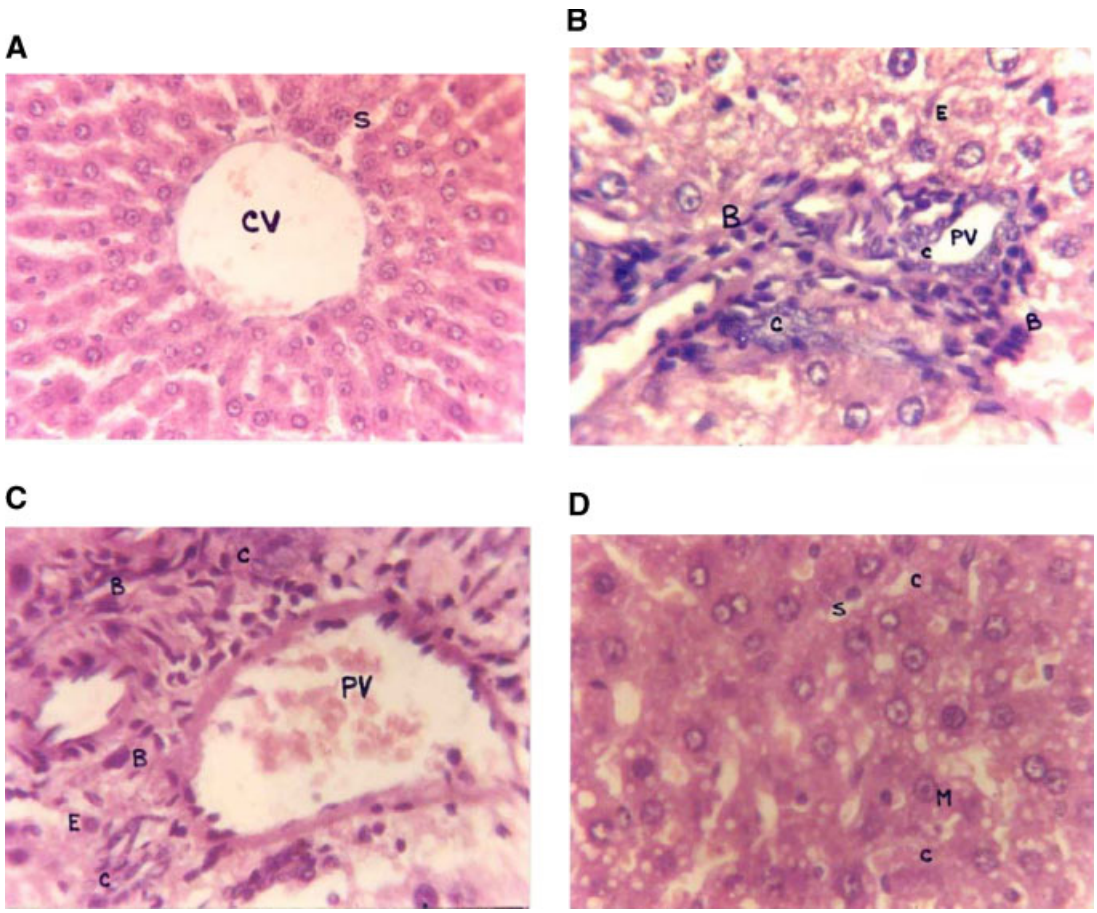

Fig. 2. Contiguous liver sections of rat showing (**A**) normal hepatocellular architecture (Group A, normal control) depicting hepatocytes radiating from the central vein; (**B**, **C**) abnormal hepatocellular histology (Group B, 2-AAF control) with prominent hyperbasophilic preneoplastic focal lesions and the presence of eosinophilic and clear cell foci after 28 weeks of chronic 0.05% 2-AAF administration; (**D**) almost normal hepatocellular architecture (Group D, vanadium + 2-AAF) after 28 weeks of chronic 0.05% 2-AAF feeding along with supplementation of 0.5 ppm vanadium starting the application four weeks before 2-AAF challenge and continued thereafter. B, basophilic foci; CV, central vein; C, clear cell foci; E, eosinophilic cell; M, mixed cell; PV, portal vein; S, sinusoid. Magnification (A–D) hematoxylin and eosin (H&E) ×450. [Color figure can be viewed in the online issue, which is available at www.interscience.wiley.com.]

observed in the carcinogen control group (Group B), which was significantly greater ($P < 0.01$) in comparison with the normal control (Group A) (Fig. 4A). Similarly, there was a significant increase in the frequency of tailed DNA ($P < 0.0001$) compared to the normal counterpart (Fig. 4B). After a short-term treatment with vanadium, the L:W ratio of DNA mass ($P < 0.05$; 57.15%) and the mean frequency of tailed DNA ($P < 0.02$; 29.55%) in the treatment group (Group D) were reduced in comparison to the carcinogen control.

Changes in MT Immunopositivity and KI at Sequential Time Points and Their Modulation by Vanadium

In situ, immunolocalization of MT protein and Ki-67 nuclear antigen was observed in 2-AAF control liver tissue showing a strong immunoreactivity (Fig. 5A,B; Fig. 7A, respectively) in comparison to that of normal control (Figure not shown). Generally, in sections with high MT immunopositivity, the immunopositive cells formed contiguous foci or sheets and on some occasions isolated clusters of positive cells were seen. Accordingly, an interesting feature of MT immunoexpression was noticed herein (Fig. 5B), which showed an intense staining of MT protein around the portal vein of the preneoplastic lesions indicating its prominent focal expression. In comparison to carcinogen control, sections from vanadium treated rat liver (Group D) (Fig. 5C) showed a low MT immunoreactivity with scattered positive cells. Figure 7A showed an intense staining of Ki-67 positive nuclei depicting its focal expression as well as

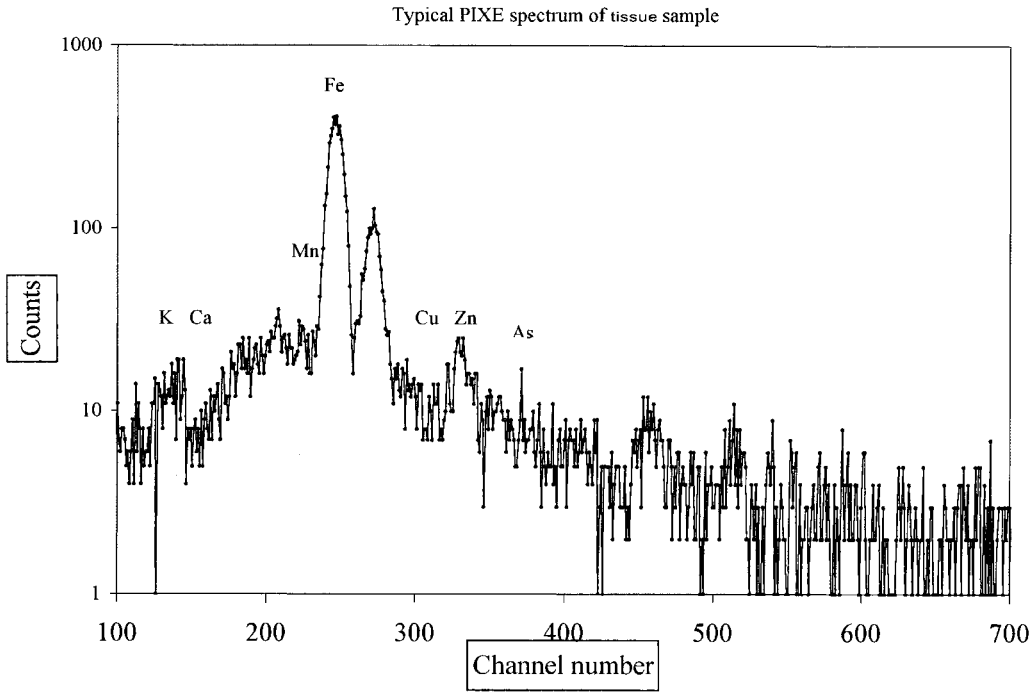

Fig. 3. Typical PIXE spectrum of vanadium treated liver tissue of rat (Group D) after 28 weeks of chronic 2-AAF exposure.

plenty of immunopositive cells throughout. However, in vanadium-treated section (Fig. 7B) no prominent focal expression was noticed.

One-way ANOVA followed by Tukey–Kramer multi-comparison test showed a significant increasing trend in both MT immunoreactivity [$P < 0.0001$; computed F is much more greater than the critical $F_{0.05\ (2.966)}$ which amounts to 15.472 (Table not shown)] and KI [$P = 0.0489$; computed F is marginally higher than the critical $F_{0.05\ (2.966)}$ which amounts to 2.969 (Table not shown)] during the 4 sequential time points studied herein (i.e., after 8, 16, 24, and 32 weeks of starting the experiment at 0 week) in 2-AAF control rat liver. At same time points, treatment with vanadium showed a prominent suppressive effect on MT immunopositivity ($P < 0.02$ at week 8 and $P < 0.05$ at 16, 24, and 32 weeks; Fig. 6) and KI ($P < 0.01$ at week 16 and $P < 0.05$ at 8, 24, and 32 weeks; Fig. 8) when compared with 2-AAF control. This was further supported by immunohistological images (Fig. 5C and Fig. 7B for MT and Ki-67 expressions, respectively).

Effect of Vanadium on p53 Expression and AI

A few p53 immunopositive cells ($0.36 \pm 0.07\%$) was detected in 2-AAF control liver

TABLE III. Effect of Vanadium on the Hepatic Contents of Zn, Mg, Se, Cu, Fe, and Ca in Different Groups of Rats With or Without 2-AAF Challenge (Killed After 32 Weeks)

Hepatic contents (μg/g of dry wt.)	Normal (Group A)	2-AAF control (Group B)	Vanadium control (Group C)	Vanadium + 2-AAF (Group D)
Zn	354.68 ± 33.28[a]	108.27 ± 12.17*	360.83 ± 25.78	287.46 ± 42.89***
Mg	197.79 ± 25.90	46.09 ± 6.54*	195.57 ± 24.38	171.98 ± 15.63***
Se	19.25 ± 2.78	3.48 ± 0.62*	18.39 ± 2.72	12.51 ± 4.12†
Cu	28.75 ± 4.21	164.05 ± 17.51*	24.65 ± 5.06	36.58 ± 5.89***
Fe	1468.12 ± 159.28	3221.38 ± 529.52**	1398.79 ± 147.74	2032.3 ± 171.22‡
Ca	2024.61 ± 194.22	3236.90 ± 123.86**	2520.41 ± 174.27	5569.85 ± 387.98***

[a]Values represent mean ± SE (n = 10).
*$P < 0.0001$ when compared to normal control (Group A).
**$P < 0.001$ when compared to normal control (Group A).
***$P < 0.0001$ when compared to 2-AAF control (Group B).
†$P < 0.05$ when compared to 2-AAF control (Group B).
‡$P < 0.001$ when compared to 2-AAF control (Group B).

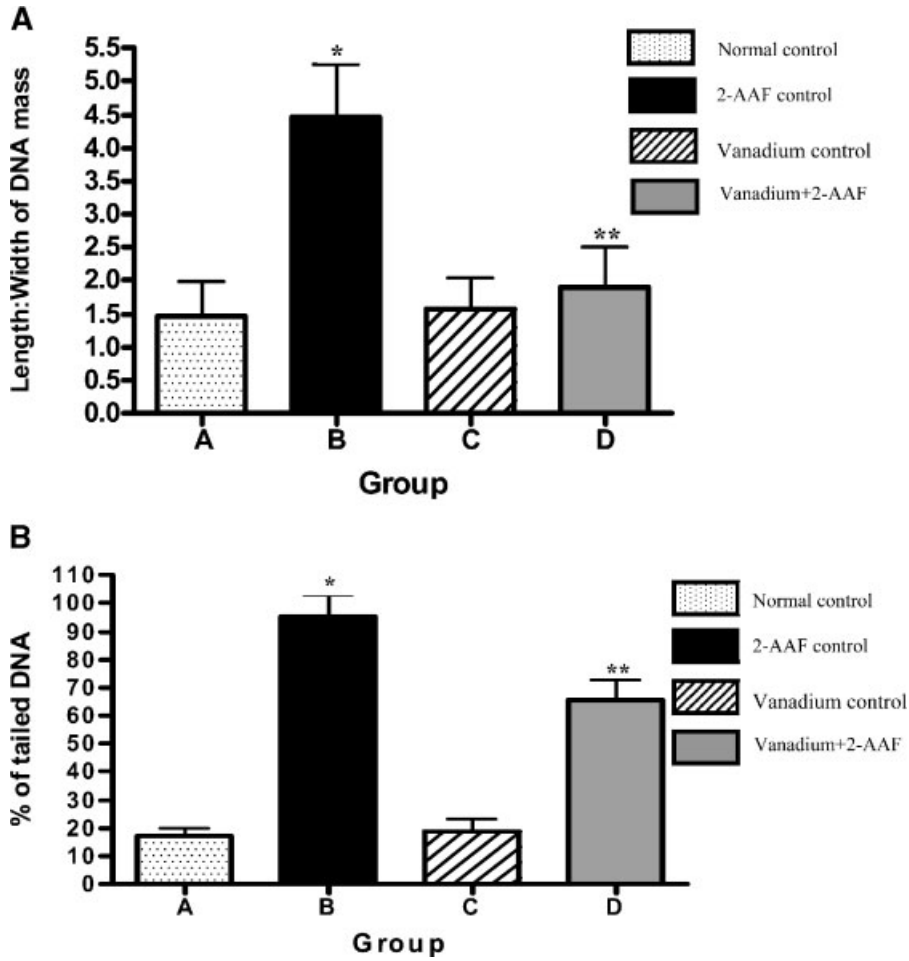

Fig. 4. Effect of vanadium (0.5 ppm) on the (**A**) length:width (L:W) of DNA mass and (**B**) percentage of tailed DNA in different groups of rat liver after 40 days from the starting of the experiment. Each column and bar indicates mean ± SE. *, $P < 0.01$ (**A**) and *, $P < 0.0001$ (**B**) when compared with normal control; **, $P < 0.05$ (**A**) and **, $P < 0.02$ (**B**) when compared with 2-AAF control.

sections (Fig. 9A), whereas Figure 9B showed an increase in p53 immunoreactivity ($1.03 \pm 0.23\%$; $P < 0.02$) upon vanadium supplementation in Group D when compared to 2-AAF control. Apoptotic cells were not detected in the normal control liver sections. The AI ranged from 0.00% to a maximum of 3.80% in the carcinogen control groups at various time points. However, there was a significant increase ($P < 0.001$ at 24 and 32 weeks) in the percentage of apoptotic cells in the vanadium-supplemented rats (Group D) as compared to that of 2-AAF control (Fig. 10).

Relationship Between MT Expression and KI

The percentage of MT-positive cells and Ki-67 immunopositivity (KI) in the tissues of 2-AAF control rats (Group B) ranged from 7.94% to 93.60% and 10.34% to 79.40%, respectively over the various time points throughout the study. A significant positive correlation was observed between MT protein expression and KI at different time intervals (Table IV) reaching a maximum positivity at week 32 (Fig. 11).

Relationship Between MT Expression and AI

The percentage of MT-positive cells and TUNEL-positive apoptotic cells (AI) in the tissues of vanadium + 2-AAF treated rats (Group D) ranged from 9.54% to 91.32% and 0.10% to 4.10%, respectively, over the various time points throughout the study. A significant negative correlation was observed between MT protein expression and AI at different time intervals in both the groups, i.e., in Groups B and D (Table IV) reaching a maximum inverse relationship at week 24 (Fig. 12A,B).

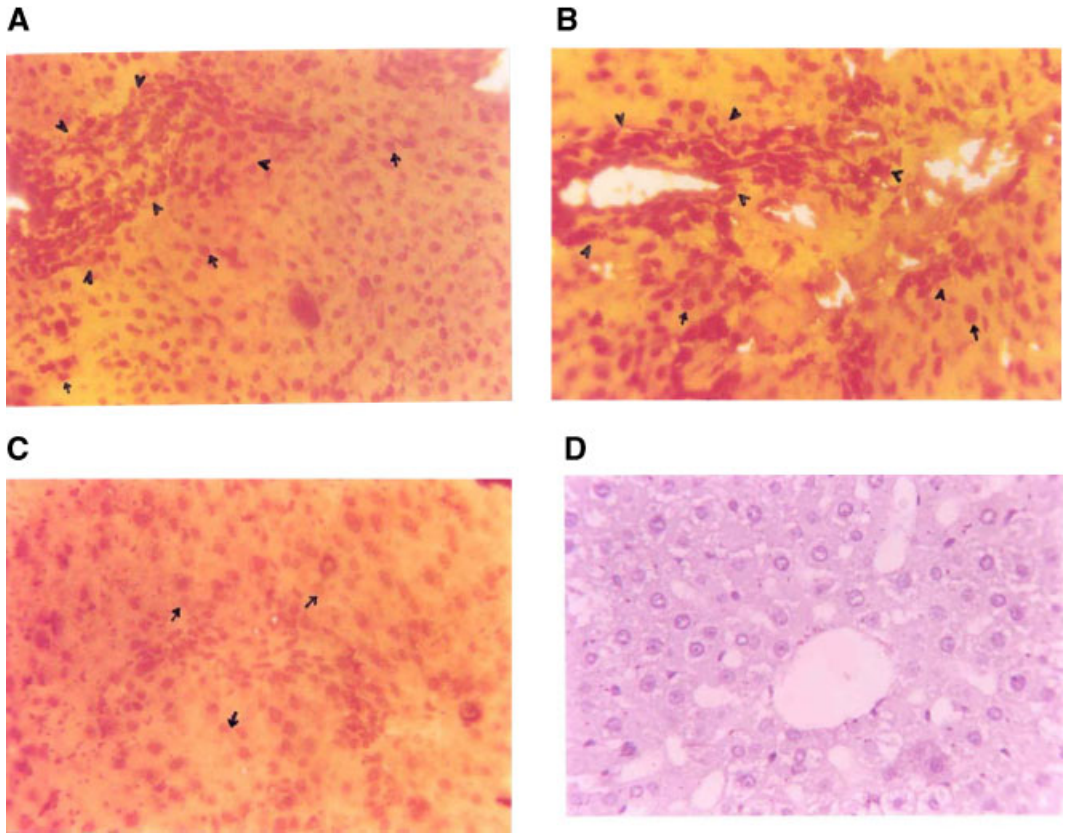

Fig. 5. Light micrographs of tissue sections from rat liver (after 32 weeks) showing immunostaining of metallothionein (MT) (**A**–**C**) with antirat MT-1 antibody and DAB; A and B (Group B, 2-AAF control); C (Group D, vanadium + 2-AAF); D (negative control). Arrow head (▲) indicates intense immunostaining of MT protein with prominent focal expression and clusters of MT-positive foci. Arrow (↑) indicates scattered MT immunopositive cells. Magnification (A–D) ×270. [Color figure can be viewed in the online issue, which is available at www.interscience.wiley.com.]

DISCUSSION

The present study demonstrates a potential role of vanadium in abating the expressions of MT and Ki-67 during 2-AAF-induced experimental hepatocarcinogenesis at various time intervals. Vanadium has also been found to induce p53 expression and apoptosis in carcinogen-challenged rat hepatocytes. Vanadium supplementation at 0.5 ppm dosage restores tissue levels of essential trace elements viz., Zn, Mg, Se, Cu, Fe, and Ca and suppresses DNA-strand breaks, thereby decreasing hepatic nodulogenesis with subsequent expression of premalignant phenotype in rat liver.

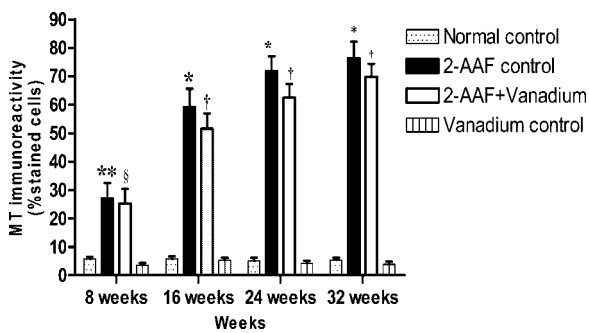

Fig. 6. Effect of vanadium (0.5 ppm) on MT immunoreactivity (% of stained cells) in 2-AAF challenged-rat liver at various time points. Each column and bar indicates mean ± SE. **, $P < 0.01$ and *, $P < 0.0001$ when compared with normal control; §, $P < 0.02$ and †, $P < 0.05$ when compared with 2-AAF control.

Supplementation of 0.5 ppm vanadium in drinking water throughout the study prominently declined the development of visible persistent nodules (PNs) and a smaller number of nodules per nodule-bearing rat liver when compared to 2-AAF-control rats. It also reduced the size of PNs by more than 3 mm in diameter. Even though, not all the hepatocyte nodules become malignant during the life span of the animals, numerous observations support the concept that the hyperplastic/neoplastic

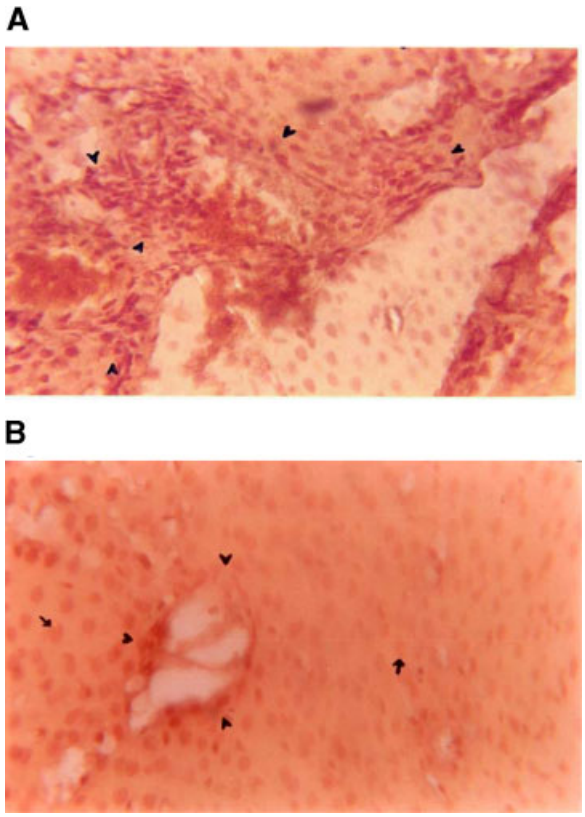

Fig. 7. Light micrographs of tissue sections from rat liver (after 32 weeks) showing immunostaining of Ki-67 [**A**: Group B, 2-AAF control; **B**: Group D, vanadium + 2-AAF] with mouse antirat Ki-67 antibody and DAB; arrow head (▲) indicates intense immunostaining of Ki-67 nuclear antigen with prominent focal expression. Arrow (↑) indicates Ki-67 immunopositive cells. Magnification (A and B) ×270. [Color figure can be viewed in the online issue, which is available at www.interscience.wiley.com.]

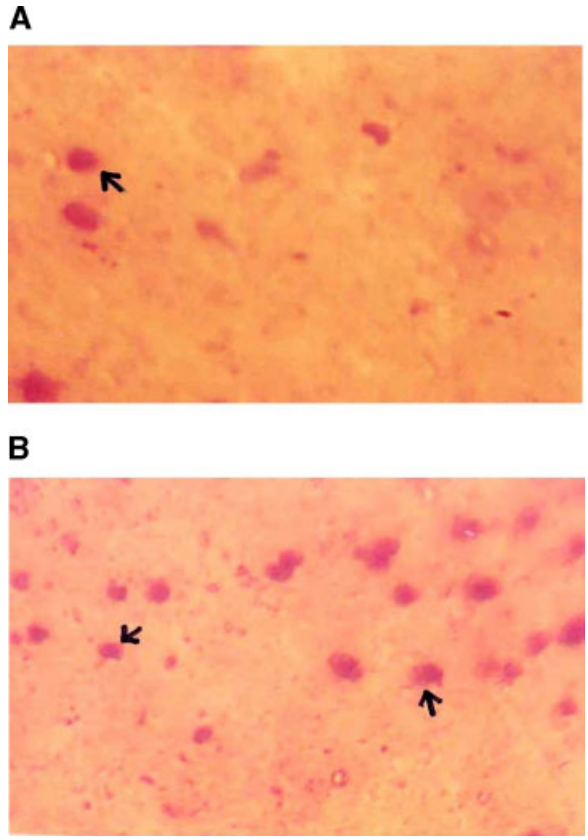

Fig. 9. Light micrographs of tissue sections from rat liver (after 32 weeks) showing immunostaining of p53 [**A**: Group B, 2-AAF control; **B**: Group D, vanadium + 2-AAF] with sheep anti-p53 antibody and DAB; arrow (↑) indicates p53 immunopositive cells. Magnification (A and B) ×270. [Color figure can be viewed in the online issue, which is available at www.interscience.wiley.com.]

nodules are the precursors of HCC [Farber and Cameron, 1980]. In view of this, inhibition of nodule incidence and enhancement of their regression by supplementary vanadium, as observed in our study may be important for cancer chemoprevention. This could be explained in the light of the fact that although the precursor lesions were still present in the

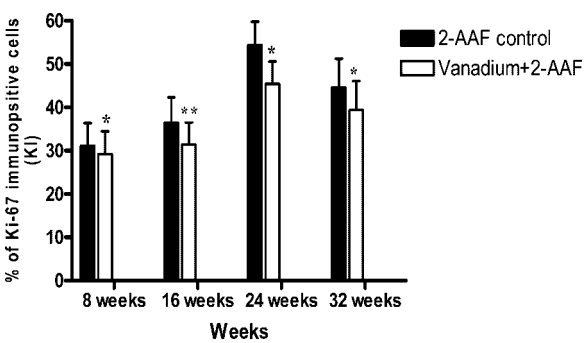

Fig. 8. Effect of vanadium (0.5 ppm) on Ki-67 immunolabeling index (KI) (% of Ki-67 immunopositive cells) in 2-AAF-challenged rat liver at various time points. Each column and bar indicates mean ± SE. *, $P < 0.05$ and **, $P < 0.01$ when compared with 2-AAF control.

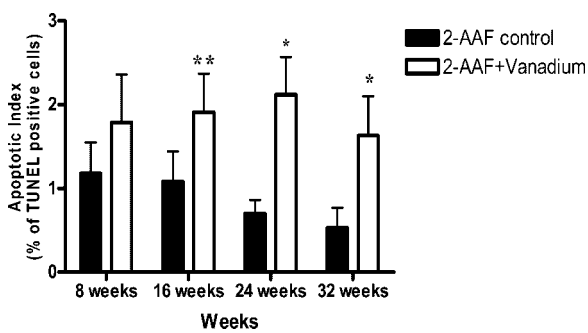

Fig. 10. Effect of vanadium (0.5 ppm) on apoptotic-index (AI) (% of TUNEL-positive cells) in 2-AAF-challenged rat liver at various time points. Each column and bar indicates mean ± SE. **, $P < 0.05$ and *, $P < 0.001$ when compared with 2-AAF control.

TABLE IV. Correlation Coefficient and Statistical Significance Between MT Immunopositivity and Ki-67 Labeling Index (KI) or Apoptotic Index (AI)

Time points (weeks)	Treatment(s)	MT versus KI		MT versus AI	
		r	*P*	*r*	*P*
8	2-AAF control	0.8280	0.01	−0.7364	0.03
	Vanadium + 2-AAF	ns	ns	−0.7100	NS
16	2-AAF control	0.8749	0.004	−0.7258	0.04
	Vanadium + 2-AAF	ns	ns	−0.9496	0.0003
24	2-AAF control	0.8749	0.004	−0.8521	0.007
	Vanadium + 2-AAF	ns	ns	−0.9000	0.0004
32	2-AAF control	0.8500	0.006	−0.8052	0.01
	Vanadium + 2-AAF	ns	ns	−0.8300	0.01

r, Pearson's correlation coefficient; ns, not shown; NS, not significant.
[In case of vanadium + 2-AAF group for MT vs. KI, statistical interpretation can be drawn from Figures 6 and 8].

livers of vanadium treated rats, their growth rates slowed to such an extent that appearance of PNs was delayed beyond the experimental end point owing to an increased latency period [Farber, 1990].

Histopathological images clearly indicate that the hyperplastic-nodular hepatocytes formed solid aggregates of one or more cells thick, the prominent "hyperbasophilic focal lesion" mainly around the portal vein in 2-AAF control rats. Different types of altered hepatocytes can be identified in the neoplastic nodules of rat. The clear and acidophilic cells primarily form "altered hepatocyte foci" (AHF) which are considered to be the small "preneoplastic focal lesions" that leads to malignant transformation in later stages of carcinogenesis with the formation of neoplastic nodules and ultimately HCCs [Peraino et al., 1981]. Thus, the majority of the neoplastic nodules consist of a mixture of preneoplastic, truly neoplastic and diverse intermediate cells. Long-term vanadium treatment

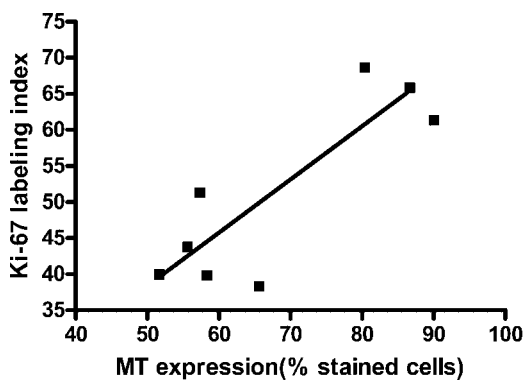

Fig. 11. Positive correlation between MT immunoreactivity (expressed as percentage of stained cells) with Ki-67 KI in 2-AAF control rat liver at 32 weeks ($r = 0.85$; $r^2 = 0.72$; $P = 0.006$).

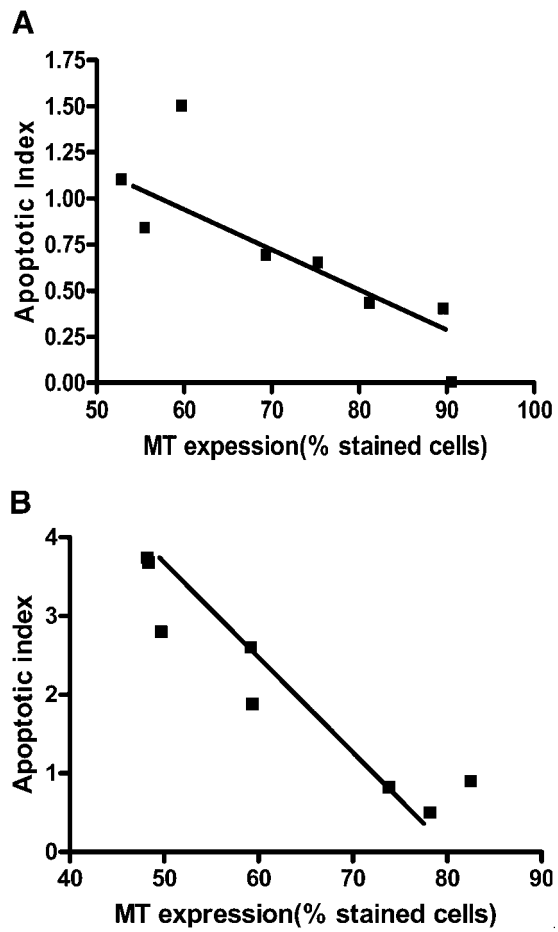

Fig. 12. Inverse relationship between MT immunoreactivity (expressed as percentage of stained cells) with apoptotic index (AI) in (**A**) 2-AAF control rat liver at 24 weeks ($r = -0.85$; $r^2 = 0.72$; $P = 0.007$) and (**B**) vanadium treated rat liver at 24 weeks ($r = -0.90$; $r^2 = 0.89$; $P = 0.0004$).

resulted in reduced hepatocyte aggregation and basophilicity with a reversal of heterogeneity towards normal cytology.

PIXE profile showed a significant reduction in the tissue levels of Zn, Mg, and Se and elevations in hepatic levels of Cu and Fe in rats belonging to the carcinogen control group. Mechanistically, Zn, Mg, and Se are known to be involved in the process of genomic stability and gene expression in a variety of ways and tissue levels of these elements are critical in the regulation of chromatin maintenance, cell-cycle progression, DNA repair, and programmed cell death and for the expression of a pathology, thereby. MT acts as a sensor of cellular redox such that a shift to more-oxidizing conditions leads to release of zinc, whereas a shift to a more-reducing environment leads to binding of zinc [Maret and Vallee, 1998]. Generation of free-radical species and reactive electrophiles upon chronic carcinogen challenge releases Zn^{2+} from MT during the initial stages of hepatocellular preneoplasia. This released Zn in turn triggers cell replication machinery by virtue of its potential to act as essential enzymatic cofactor and furthermore, acts as a feedback signal to induce MT gene transcription [Katakai et al., 2001]. Thus, a constitutive/elevated expression of MT results in the production of Zn-sequestering-apo-T (Thionein), a metal-free state, that, with the passage of time possibly generates a Zn-limiting cellular environment [St. Croix et al., 2002]. Decrease in intracellular Mg in rat liver showed an increased susceptibility to oxidative stress and their tissues were more sensitive to peroxidation resulting in altered membrane functions, perturbations of intracellular calcium metabolism and increased DNA-strand breaks [Dickens et al., 1992]. Cell proliferation and cell-cycle proteins have been proposed as targets against which Se exerts its action in limiting cell growth. A marked reduction in Se content has been linked with increased cell proliferation events. The sudden release of copper ions and their subsequent accumulation during the process of carcinogenesis may be related to the reduced level of Cu-binding albumin as well as due to chemical oxidation of the thiol groups on copper-containing-MT [Fabisiak et al., 1999]. Iron, though vital in life-processes is also potentially toxic to living cells due to its ability to exist in two stable and inter-convertible redox-active states, since redox reactions catalyze the formation of oxyradicals generating superoxide radicals (O_2^-), which is the precursor of toxic H_2O_2 [Keyer and Imlay, 1996]. Moreover, ferrous iron can reduce copper to the cuprous state, which is a more potent generator of hydroxyl radicals than ferrous ions, thus iron acts synergistically with copper in the carcinogenic process. Thus, Zn-, Mg-, and Se-deficient environment and accumulated free radicals ultimately favor DNA lesions resulting in increased hepatic cell proliferation, phenotypic transformation, and expression of neoplastic pathology with minimal apoptotic events.

Vanadium-mediated restoration of hepatic levels of Zn, Se, and Mg may have a role in the repair of DNA base-lesions in vivo. Furthermore, normalization of hepatic Cu and Fe levels minimizes the possibility of free-radical generation, thereby preventing oxidative injury to cells and DNA. Restoration of Se level after treatment with vanadium has been linked with suppression of cell proliferation events by interacting with its targets. Recent studies from our laboratory indicate that, vanadium at a low concentration, at a dose of 0.5 ppm acts as an antioxidant and maintains membrane and genomic integrity [Kanna et al., 2004].

The most important among endogenous processes causing DNA damage like reactive oxygen species (ROS) and reactive nitrogen species (RNS) are generated as a consequence of carcinogen exposure, leading to DNA-strand breaks [Halliwell and Aruoma, 1991]. For the cell, DSBs are probably the most deleterious form of DNA damage and may arise during the replication of an SSB, when carcinogen-induced SSBs remain unrepaired [Jackson, 2002]. Error-prone repair of DSBs can lead to chromosomal aberrations as well as oncogene activations that contribute to carcinogenesis. Thus, SSBs can be considered as a fundamental to the maintenance of chromosome integrity and genetic stability. In the present study, a substantial decrease in the amount of 2-AAF-induced 'tailed' DNA and DNA 'comets' by vanadium could reflect its anticlastogenic potential to combat genotoxicity.

Immunohistological impressions clearly reveal the intense immunostaining of MT in preneoplastic liver tissue over normal control. It is necessary to mention that, the hyperbasophilic cells of the preneoplastic histomorphological lesions stained more intensely for MT

compared to that of the non-basophilic area of the same tissue suggesting that, the hyperbasophilic proliferative lesions consisting of rapidly proliferating cells may be considered to be the primary MT(-positive focal) expression zones. Moreover, a time-dependent increase in MT protein expression following carcinogen exposure may be of prime importance, both clinically and experimentally for determining the stages or grades of tumor differentiation and the duration of carcinoma progression as well as in early detection, prognosis, recurrence, and diagnosis of the pathology. Thus, localized expression of MT in areas of high proliferative activities in preneoplastic lesions and alterations of expression may be an early event in the pathogenesis of hepatic neoplasia. The mechanisms leading to overexpression of MT in preneoplastic hepatic nodules are largely unknown. However, it has been shown by several researchers that MT expression is induced during any kind of cellular insultations as a protective means. Carcinogen-induced MT gene amplification may be another mechanism for the said observation [Matthias et al., 2000].

MT has been implicated in neoplastic cell growth as there have been reports indicating MT to be a cell-cycle-dependent protein. There are several possible mechanisms by which MT could exert mitogenic response. The MT protein could supply zinc ions to enzymes such as DNA and RNA polymerases, which are critical in cell replication process. There is experimental evidence that zinc ions are transferred between MT and zinc proteins [Jacob et al., 1998]. Another possibility is that MT directly interacts with transcription factors involved in the intricate signaling mechanisms that stimulate cell proliferation. Abedel-Mageed and Agrawal [1998] have found a direct interaction of MT with the p50 subunit of NF-κβ, leading to transactivation of the latter, which is a heterodimeric sequence-specific key nuclear transcriptional factor for cell growth signaling, thus supporting the concept that NF-κβ may mediate the antiapoptoic and growth-promoting effects of MT.

Expression of Ki-67 protein is another prerequisite for cell-cycle progression. Proliferation correlates with its accumulation from G_1–S–G_2-phase to mitosis, where it is found at its highest content in nuclei of proliferating cells but not in nuclei of quiescent or resting cells [Starborg et al., 1996]. The Ki-67 protein is predominantly localized in the nucleolus during interphase, whereas during mitosis it becomes associated with the periphery of the condensed chromosomes. We have found here, a significant correlation of the KI with MT protein expression, thus supporting the role of MT in cell proliferation in preneoplastic hepatic tissues as well as in other reported tumors.

Treatment with vanadium prominently reduced MT expression in carcinogen-challenged rat liver. The exact molecular mechanism of vanadium-mediated down-regulation of MT expression is not clear at the moment; however, it is implied that vanadium-mediated restoration of tissue antioxidants, as reported earlier by us [Bishayee et al., 1999; Chakraborty et al., 2003] may lead to elimination of reactive metabolites from the system, thereby posing low oxidative stress to the host and as a result of which MT is down-regulated towards the basal level. Moreover, it has been demonstrated that Zn binding is crucial for p53 protein stabilization and DNA binding [Meplan et al., 2000]. Since MT plays an important role in Zn homeostasis, vanadium-mediated down-regulation of MT may therefore be involved in the redox release of Zn, which in turn binds to and stabilizes p53 protein conformation and upregulates its tumor suppressor activity leading to tumor cell apoptosis as documented by TUNEL assay. So, there exists an inverse association between MT expression and p53 induction as well as apoptosis. In this context, one point to be noted that, vanadium was able to induce apoptosis in rat hepatocytes but abated the generation of DNA SSBs. The latter is a measure of oxidative DNA damage and thus an indicator of genotoxicity. So, it is clear from these studies that vanadium-mediated induction of apoptotic cell death, as observed herein was not a consequence of genotoxicity induced by vanadium. Thus, vanadium here acting as a non-genotoxic, apoptosis-inducing agent in rat liver preneoplasia.

Several mechanisms have been proposed for vanadium action in limiting neoplastic expression. Studies on various cell lines reveal that vanadium exerts its antitumor effects through inhibition of cellular tyrosine phosphatases and/or activation of protein tyrosine kinases [Evangelou, 2002]. Furthermore, it has been reported that this trace metal drastically reduced the mutagenicity of metabolically

activated hepatocarcinogen, 2-AAF by the modulation of protein phosphorylation [Oesch-Bartlomowicz et al., 1997]. It has also been shown that, vanadium can regulate the activity of second messengers, viz., cAMP, phosphoinositide system, and Ca^{2+} and thereby affects signal transduction in the cell [Bencherif and Lukas, 1992; Pugazhenthi and Khandelwal, 1992]. It activates phospholipase C (PLC)-coupled G-protein and consequently stimulates inositol-phosphate (IP_3) synthesis. On the other hand, vanadium directly inhibits the dephosphorylation of IP_3. The cooperation of these two events would result in increased IP_3 level that in turn acts as a signal in the mobilization of Ca^{2+} from intracellular stores such as mitochondria, ER, etc. and the subsequent increase in intracellular Ca^{2+} level. Several reports support our PIXE finding that, elevated tissue level of Ca^{2+} beyond a critical value appears to be cytotoxic and intiates apoptotic cell death [Kim et al., 2002].

Another potential mechanism of vanadium that comes out from our study is vanadium-mediated induction of p53 protein causing apoptosis. Vanadium is a well known pro-oxidant at high dosage. Continuous supplementation of 0.5 ppm vanadium may result in the generation of free radicals that has been proposed as one of the mechanisms by which this element exerts its cellular actions. Vanadium generates endogenous H_2O_2 from superoxide radicals (O_2^-) that is required for p53 transactivation and thereby apoptosis [Huang et al., 2000]. Furthermore, formation of hydroxyl radicals (OH) from accumulated H_2O_2 has been reported to cleave DNA molecule leading to cell death. This is the first report of vanadium-mediated suppression of 2-AAF-induced MT and Ki-67 expressions in rat liver preneoplasia that may interfere with cell replication machinery and induction of p53 and apoptosis as well could account for its promising role in suppressing experimental hepatocarcinogenesis. Vanadium may thus be considered as a potential cancer chemopreventive agent for the future, which warrants a detailed molecular mechanistic study.

ACKNOWLEDGMENTS

Tridib Chakraborty is highly indebted to the University Grant Commission (UGC), Government of India, for the financial assistance. A part of the total cost for this work was defrayed from the UGC Project, Government of India, [Project No. P-1/RS/34/2001; T. Chakraborty was a Research Fellow in this Project]. The authors sincerely acknowledge Prof. Jim Geiser, University of Kansas, Kansas Medical Center for providing the rat antiserum of MT as a kind gift. The authors do convey their gratitude to Dr. V. Vijayan, Institute of Physics (IOP), Bhubaneswar, India for providing the PIXE facility and extending his hand for PIXE analysis of biological samples. Generous help from Dr. P.K. Sen, Department of Mathematics, Jadavpur University, Kolkata for statistical interpretation is truly acknowledged.

REFERENCES

Abedel-Mageed AB, Agrawal KC. 1998. Activation of nuclear factor kappa B: Potential role in metallothionein-mediated mitogenic response. Cancer Res 58:335–2338.

Basak R, Saha BK, Chatterjee M. 2000. Inhibition of diethylnitrosamine-induced rat liver chromosomal aberrations and DNA-strand breaks by synergistic supplementation of vanadium and 1α,25-dihydroxyvitamin D_3. Biochim Biophys Acta 1502:273–282.

Bencherif M, Lukas RJ. 1992. Vanadate amplifies receptor-mediated accumulation of inositol triphosphates and inhibits inositol tris and tetrakis-phosphatase activities. Neurosci Lett 134:157–160.

Bishayee A, Karmakar R, Mandal A, Chatterjee M. 1997. Vanadium-mediated chemoprotection against chemical rat hepatocarcinogenesis: Reflection in hematological and histological characteristics. Eur J Cancer Prev 6:58–70.

Bishayee A, Roy S, Chatterjee M. 1999. Characterization of selective induction and alteration of xenobiotic biotransforming enzymes by vanadium during diethylnitrosamine-induced chemical rat liver carcinogenesis. Oncol Res 11:41–53.

Chakraborty T, Ghosh S, Datta S, Chakraborty P, Chatterjee M. 2003. Vanadium suppresses sister-chromatid exchange and DNA–protein crosslink formation and restores antioxidant status and hepatocellular architecture during 2-acetylaminofluorene-induced experimental rat hepatocarcinogenesis. J Exp Therp Oncol 3:346–362.

Dickens BF, Weglicki WB, Li YS, Mak T. 1992. Magnesium deficiency in vitro enhances free radical-induced intracellular oxidation and cytotoxicity in endothelial cells. FEBS Lett 311:187–191.

Evangelou AM. 2002. Vanadium in cancer treatment. Crt Rev Oncol Hematol 42:249–265.

Fabisiak JP, Pearce LL, Borisenko GG, Tyurina YY, Tyurin VA, Razzack J. 1999. Bifunctional anti/prooxidant potential of metallothionein: Redox signaling of copper binding and release. Antioxi Redox Signaling 1:349–364.

Farber E. 1990. Clonal adaptation during carcinogenesis. Biochem Pharmacol 39:1837–1846.

Farber E, Cameron R. 1980. The sequential analysis of cancer development. Adv Cancer Res 35:125–226.

Feldstein H, Cohen Y, Shenberg C, Klein A, Kojller M, Maenhaut W, Cafmeyer J, Cornelis R. 1998. Comparison

between levels of trace elements in normal and cancer inoculated mice by XRF and PIXE. Biol Trace Elem Res 61:169–180.

Fenech M, Ferguson LR. 2001. Vitamins/minerals and genomic stability in humans. Mutat Res 475:1–6.

French RJ, Jones PJ. 1993. Role of vanadium in nutrition: Metabolism, essentiality, and dietary consideration. Life Sci 52:339–346.

Gavrieli Y, Sherman Y, Ben-Sasson SA. 1992. Identification of programmed cell death in situ via specific labeling of nuclear DNA fragmentation. J Cell Biol 119:493–501.

Halliwell B, Aruoma OI. 1991. DNA damage by oxygen-derived species. Its mechanism and measurement in mammalian cells. FEBS Lett 281:9–19.

Hota PK, Vijayan V, Singh LP. 2001. Application of X-ray spectroscopic analysis to human blood samples. Ind J Phys 75B:333–336.

Huang GW, Yang LY. 2002. Metallothionein expression in hepatocellular carcinoma. World J Gastroenterol 8:650–653.

Huang C, Zhang Z, Ding M, Li J, Ye J, Leonard SS, Shen HM, Butterworth L, Lu Y, Costa M, Rojanasakul Y, Castranova V, Vallyathan V, Shi X. 2000. Vanadate Induces p53 transactivation through hydrogen peroxide and causes apoptosis. J Biol Chem 275:32516–32522.

Ito Y, Matsuura N, Sakon M, Takeda T, Umeshita K, Nagano H, Nakamori S, Dono K, Tsujimoto M, Nakahara M, Nakao K, Monden M. 1999. Both cell proliferation and apoptosis significantly predict shortened disease-free survival in hepatocellular carcinoma. Br J Cancer 81: 747–751.

Jackson SP. 2002. Sensing and repairing DNA double-strand breaks. Carcinogenesis 23:687–696.

Jacob C, Maret W, Vallee BL. 1998. Control of zinc transfer between thionein, metallothionein and zinc proteins. Proc Natl Acad Sci USA 95:3489–3494.

Jayasurya A, Bay BH, Yap WM, Tan NG, Tan BKH. 2000. Proliferative potential in nasopharyngeal carcinoma: Correlations with metallothionein expression and tissue zinc levels. Carcinogenesis 21:1809–1812.

Jin R, Chow VTK, Tan PH, Dheen ST, Duan W, Bay BH. 2002. Metallothionein 2A expression is associated with cell proliferation in breast cancer. Carcinogenesis 23: 81–86.

Kanna PS, Mahendrakumar CB, Indira BN, Srivastawa S, Kalaiselvi K, Elayaraja T, Chatterjee M. 2004. Chemopreventive effect of vanadium towards 1,2 dimethylhydrazine induced genotoxicity and preneoplastic lesions in rat colon. Environ Mol Mutagen 44:113–118.

Katakai K, Liu J, Nakajima K, Keefer LK, Waalkes MP. 2001. Nitric oxide induces metallothionein (MT) gene expression apparently by displacing zinc bound to MT. Toxicol Lett 119:103–108.

Keyer K, Imlay A. 1996. Superoxide accelerates DNA damage by elevating free-iron levels. Proc Natl Acad Sci USA 93:13635–13640.

Kim BC, Kim HT, Mamura M, Indu S, Choi KS, Kim SJ. 2002. Tumor necrosis factor induces apoptosis in hepatoma cells by increasing Ca^{2+} release from the endoplasmic reticulum and suppressing Bcl-2 expression. J Biol Chem 277:31381–31389.

Kopf-Maier P, Kopf H. 1988. Transition and main-group metal cyclopentadienyl complexes: Preclinical studies on a series of antitumor agents of different structural type. Struct Bond 70:103–185.

Kwiatek WM, Cholewa M, Kajfosz J, Jones KW, Shore RE, Redrick AL. 1987. Correlation of trace elements in hair of patients with colon cancer. Nucl Instrum Methods Phys Res B22:166–171.

Lindahl T. 1993. Instability and decay of the primary structure of DNA. Nature 362:709–715.

Maret W, Vallee BL. 1998. Thiolate ligands in metallothionein confer redox activity on zinc clusters. Proc Natl Acad Sci USA 95:3478–3482.

Matthias PAE, Gunther T, Hoffmann J, Yu J, Michlke S, Schulz HU, Roessner A, Kore M, Malferpheiner P. 2000. Expression of metallothionein II in intestinal metaplasia, dysplasia, and gastric cancer. Cancer Res 60:1995–2001.

Maxwell JA, Teesdale WJ, Campbell JL. 1995. The Guelph PIXE software package II. Nucl Inst Meth B95:407–409.

Meplan C, Richard MJ, Hainaut P. 2000. Metalloregulation of the tumor suppressor protein p53: Zinc mediates the renaturation of p53 after exposure to metal chelators in vitro and in intact cells. Oncogene 19:5227–5236.

Moreno FS, Rizzi MBSL, Dagli MLZ, Penteado MVC. 1991. Inhibitory effect of β-carotene on preneoplastic lesions induced in Wistar rats by the resistant hepatocyte model. Carcinogenesis 12:1817–1822.

Murthy MS, Rao LN, Kuo LY, Toney JH, Marks TJ. 1988. Antitumor and toxicologic properties of the organometallic anticancer agent vanadocene dichloride. Inorg Chim Acta 152:117–124.

Oesch-Bartlomowicz B, Arnes HJ, Richter B, Hengstler JG, Oesch F. 1997. Control of the mutagenicity of aromatic amines by protein kinases and phosphatases. I. The protein phosphates inhibitors okadaic acid and orthovanadate drastically reduced the mutagenicity of aromatic amines. Arch Toxicol 71:601–611.

Olive PL, Wlodek D, Duran RE, Banath JP. 1992. Factors influencing DNA migration from individual cells subjected to gel electrophoresis. Exp Cell Res 198:259–267.

Oyama T, Take H, Hikino T, Lino Y, Nakajima T. 1996. Immunohistochemical expression of metallothionein in invasive breast cancer in relation to proliferative activity, histology, and prognosis. Oncology 53:112–117.

Peraino C, Staffeldt EF, Ludeman VA. 1981. Early appearance of histochemically altered hepatocyte foci and liver tumors in female rats treated with carcinogens one day after birth. Carcinogenesis 2:463–465.

Pugazhenthi S, Khandelwal RL. 1992. Vanadate increases protein kinase C-induced phosphorylation of endogenous proteins of liver in vitro. Biochem Int 26:241–247.

Qiu LM, Li WJ, Pang XY, Gao QX, Feng Y, Zhou LB, Zhang GH. 2003. Observation of DNA damage of human hepatoma cells irradiated by heavy ions using comet assay. World J Gastroenterol 9:1450–1454.

Saha BK, Bishayee A, Kanjilal NB, Chatterjee M. 2001. 1α,25-dihydroxyvitamin D_3 inhibits hepatic chromosomal aberrations, DNA strand breaks and specific DNA adducts during rat hepatocarcinogenesis. Cell Mol Life Sci 58:1141–1149.

Sakurai H, Tamura H, Okatani K. 1995. Mechanism for a new antitumor vanadium complex: Hydroxyl radical dependent DNA cleavage by 1,10-phenanthroline–vanadyl complex in the presence of hydrogen peroxide. Biochem Biophys Res Commun 206:133–137.

St. Croix CM, Wasserloos KJ, Dineley KE, Reynolds IJ, Levitan ES, Pitt BR. 2002. Nitric oxide-induced changes in intracellular zinc homeostasis are mediated by metallothionein/thionein. Am J Physiol Lung Cell Mol Physiol 282:L185–L192.

Starborg M, Gell K, Brundell E, Hoog C. 1996. The murine Ki-67 cell proliferation antigen accumulates in the nucleolar and heterochromatic regions of interphase cells and at the periphery of the mitotic chromosomes in a process essential for cell-cycle progression. J Cell Sci 109: 43–53.

Stern A, Yin X, Tsang SS, Davidson A, Moon J. 1993. Vanadium as a modulator of cellular regulatory cascades and oncogene expression. Biochem Cell Biol 71:103–112.

Symonds H, Krall L, Remington L, Saenzrobles M, Lowe S, Jacks T, Vandyke T. 1994. p53-dependent apoptosis suppresses tumor-growth and progression in vivo. Cell 78:703–711.

Tatematsu M, Nagamine Y, Farber E. 1988. Stable phenotypic expression of glutathione-S-transferase placental type and unstable phenotypic expression of γ-glutamyl transpeptidase in rat liver preneoplastic and neoplastic lesions. Carcinogenesis 9:215–220.